Supporting Information

Bukiya et al. 10.1073/pnas.1317363111

SI Materials and Methods

Protein Homology Model Generation and Validation. Protein homology modeling and validation of the resulting homology models were performed by Molecular Operating Environment software (MOE, Chemical Computing Group) (1–3). Before the homology modeling, the mslo1 amino acid sequence (protein homolog) was aligned with hslo1 (template). This alignment demonstrated ~99% identity in amino acid sequence between mslo1 and hslo1, highlighting appropriate choice of the protein template. Homology modeling routine was run using built-in function in MOE. During homology modeling based on either 3MT5 or 3NAF template, 10 initial models where generated. Amber 99 forcefield was used, with dielectric constant of the exterior solvent set to 80 to mimic aqueous environment of the cytosolic part of the protein. For each template, out of 10 intermediate models the final model was chosen based on the best-scoring intermediate model measured as electrostatic solvation energy by Generalized Born/Volume Integral (GB/VI) methodology (4).

The final models were further checked for unusual or unreasonable features using Ramachandran plot generation in MOE. Compared with template geometry of 3MT5, final homology model possessed reasonable structural features with only 5 individual amino acid outliers. For 3NAF5 template, final homology model contained only 14 amino acid outliers. In both homology models, pointed amino acid outliers were located away from the proposed alcohol-sensing regions.

Mutagenesis and Expression. cDNAs coding for mouse brain slo1 (mslo1; mbr5) inserted into the pBluescript vector were cut with ClaI and NotI and reinserted into the pBscMXT vector for expression in *Xenopus laevis* oocytes. Mslo1 mutants were constructed using QuikChange site-directed mutagenesis kit (Stratagene). Desired mutations and lack of unwanted mutations were confirmed by sequencing at the University of Tennessee Molecular Research Center. Mslo cDNAs were linearized with SalI (New England Biolab) and transcribed in vitro using T3 polymerase (Ambion).

Oocytes were removed and defolliculated as described (5). The care of animals and experimental protocols were reviewed and approved by the Animal Care and Use Committee of the University of Tennessee Health Science Center, which is an institution accredited by the Association for Assessment and Accreditation of Laboratory Animal Care. Defolliculated oocytes were transferred to ND-96 solution: 82.5 mM NaCl, 1 mM $MgCl_2$, 2 mM KCl, 1.8 mM $CaCl_2$, and 5 mM Hepes; pH 7.4, supplemented with 2.5 mM pyruvate. Penicillin-streptomycin solution (Cellgro) was added to ND-96 to render 10,000 IU of penicillin and 10 mg of streptomycin per 500 mL (6). Mslo mbr5 cRNA (10–30 ng/μL) was injected at 23 nL per oocyte using a modified micropipette (Drummond Scientific). The interval between cRNA injection and patch-clamping was 36–48 h. During this time, injected oocytes were kept at +15 °C.

Electrophysiology Data Acquisition and Analysis. Oocytes were prepared for patch-clamp recording as described (5). Currents were recorded from I/O patches. Both bath and electrode solutions contained: 130 mM K^+ gluconate, 5 mM EGTA, 2.28 mM $MgCl_2$, 15 mM Hepes, 1.6 mM HEDTA; pH 7.35. In all experiments, free $Ca^{2+}{}_i$ in solution was adjusted to the desired value by adding $CaCl_2$. When desired free $Ca^{2+}{}_i$ did not exceed 1 μM, HEDTA was omitted from the solution, and final $MgCl_2$ was set to 1 mM. In all cases, nominal free $Ca^{2+}{}_i$ was calculated with MaxChelator Sliders (C. Patton, Stanford University, Stanford, CA) and validated experimentally using $Ca^{2+}{}_i$-selective electrodes (Corning) (7).

Patch-clamp electrodes were pulled from glass capillaries (Drummond Scientific). Immediately before recording, the tip of the electrode was fire-polished on a microforge (World Precision Instruments) to give resistances of 8–10 MΩ when filled with extracellular (electrode) solution. An agar bridge with gluconate as the main anion was used as ground electrode. After excision from the cell, the membrane patch was exposed to a stream of bath solution with or without ethanol. Urea iso-osmotically substituting for ethanol in bath solution was used as control perfusion. Solutions were applied onto the patch cytosolic side using a pressurized, automated DAD12 system (ALA Scientific Instruments) via a micropipette tip with an internal diameter of 100 μm. Experiments were carried out at room temperature (20–22 °C).

Ionic current was recorded using an EPC8 amplifier (HEKA) at 1 kHz. Data were digitized at 5 kHz using a Digidata 1320A A/D converter and pCLAMP 8.0 (Molecular Devices). The product of number of channels in the patch (N) and channel open probability (Po) was used as an index of channel steady-state activity. NPo was obtained using a built-in option in Clampfit 9.2 (Molecular Devices) from ≥1 min of gap-free recording under each condition.

With exception of data obtained at 0.3 μM $Ca^{2+}{}_i$ (Fig. S3), macroscopic ionic currents were evoked from a holding potential of −80 mV by 200-ms-long, 10-mV steps ranging from −150 to +150 mV. Current amplitude was obtained from steady-state ionic current at 100–150 ms after initiation of the voltage pulse. Macroscopic conductance $G/G_{max} - V$ plots were fitted to a Boltzmann function of the type $G(V) = G_{max}/1 + \exp[(-V + V_{half})/k]$. The fitting allows us to obtain V_{half}, and k; the former is the voltage needed to reach half-maximal macroscopic current (conductance), whereas k represents the slope of the curve, which is determined from the following equation: slope = zF/RT. In this equation, z is effective valance, F = 96,485 C/mol, R = 8.31 J/(mole*K), T = absolute temperature. Boltzmann fitting routines were run using the Levenberg–Marquardt algorithm to perform nonlinear least squares fits.

Chemicals. Ethanol (100% purity) was purchased from American Bioanalytical. All other chemicals were purchased from Sigma-Aldrich. Alkanols from ethanol to heptanol were directly dissolved to desired concentration in bath recording solution. For hexanol, heptanol, and octanol, ethanol was used as a vehicle, the ethanol final concentration in the perfusion solution ≤ 8 mM (8), which was also used as control perfusion for the last three alkanols tested.

Data Analysis. Final plotting, fitting and statistical analysis of data were conducted using Origin 8.5.1 (OriginLab) and InStat 3.0 (GraphPad). Statistical analysis was conducted using either one-way ANOVA and Bonferroni's multiple comparison test or Student t test, according to experimental design. Significance was set at $P < 0.05$. Data are expressed as mean ± SEM; n = number of patches. Each patch was obtained from a different oocyte.

1. Al-Moubarak E, Simons C (2011) A homology model for Clostridium difficile methionyl tRNA synthetase: Active site analysis and docking interactions. *J Mol Model* 17(7):1679–1693.

2. Dolan MA, Noah JW, Hurt D (2012) Comparison of common homology modeling algorithms: Application of user-defined alignments. *Methods Mol Biol* 857:399–414.

3. Yamaguchi H, Kidachi Y, Kamiie K, Noshita T, Umetsu H (2012) Homology modeling and structural analysis of human P-glycoprotein. *Bioinformation* 8(22):1066–1074.
4. Labute P (2008) The generalized Born/volume integral implicit solvent model: Estimation of the free energy of hydration using London dispersion instead of atomic surface area. *J Comput Chem* 29(10):1693–1698.
5. Bukiya AN, et al. (2013) Cerebrovascular dilation via selective targeting of the cholane steroid-recognition site in the BK channel β1-subunit by a novel nonsteroidal agent. *Mol Pharmacol* 83(5):1030–1044.
6. Colville CA, Gould GW (1994) Expression of membrane transport proteins in *Xenopus* oocytes. *Membrane Protein Expression Systems: A User's Guide*, ed Gould GW (Portland Press, London), p 250.
7. Dopico AM (2003) Ethanol sensitivity of $BK_{(Ca)}$ channels from arterial smooth muscle does not require the presence of the beta 1-subunit. *Am J Physiol Cell Physiol* 284(6):C1468–C1480.
8. Chu B, Treistman SN (1997) Modulation of two cloned potassium channels by 1-alkanols demonstrates different cutoffs. *Alcohol Clin Exp Res* 21(6):1103–1107.

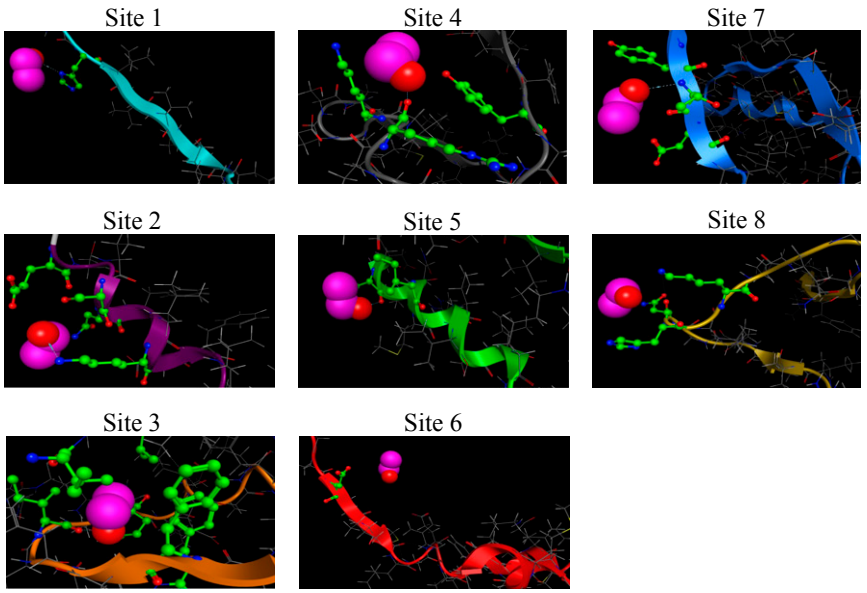

Fig. S1. The representative screenshots of the multifragment search results at each alcohol-sensing region of mslo1 CTD. Ethanol molecule is depicted in pink; proposed amino acid residues interacting with ethanol are in green, hydrogen bonding is indicated by a dotted line. In each snapshot, protein backbone is color-coded according to colors assigned to proposed alcohol-sensing regions in Fig. 1.

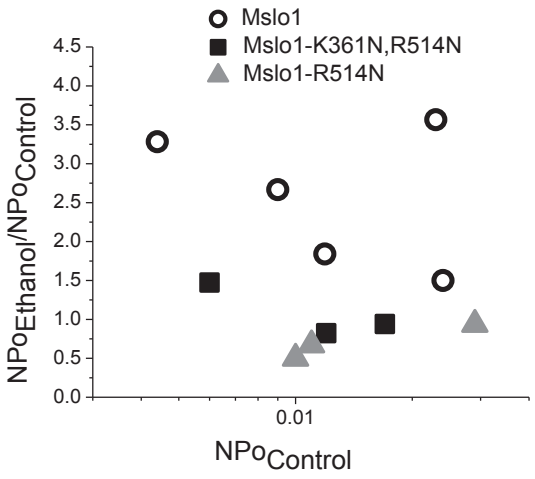

Fig. S2. Ethanol-induced increase in mslo1, mslo1-K361N,R514N, or mslo1-R514N channel NPo shows no correlation with the corresponding basal NPo. A semilog scatter graph of ethanol response (as ratio of NPo in presence and absence of 100 mM ethanol) as function of basal (pre-ethanol) NPo is shown.

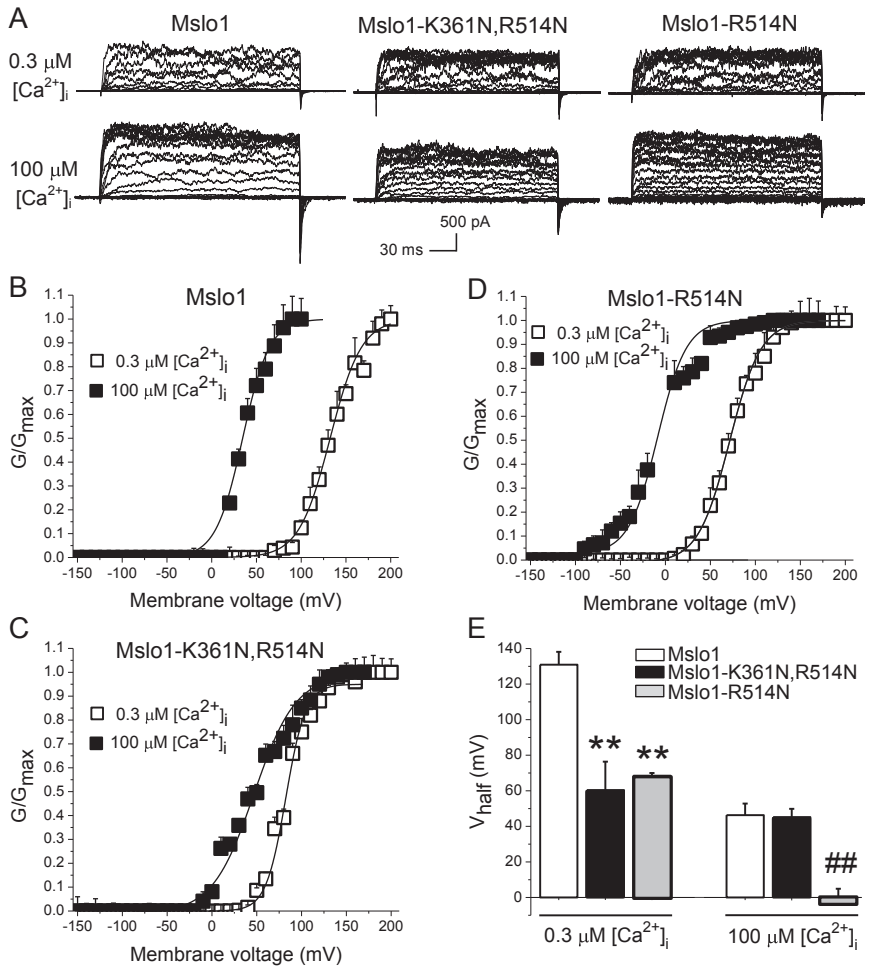

Fig. S3. Constructs that include the R514N substitution modify the channel's apparent Ca^{2+} sensitivity. (*A*) Macroscopic currents from oocyte membrane I/O patches expressing WT mslo1, mslo1-K361N,R514N, or mslo1-R514N, and exposed to 0.3 and 100 μM $Ca^{2+}{}_i$. Here and in Fig. S4, patches were held at −80 mV and stepped from −150 to 150 mV at 10 mV increments. At 0.3 μM $Ca^{2+}{}_i$, however, patches were stepped from −150 to 200 mV to reach saturation of ionic current. $G/G_{max} - V$ plots from mslo1 (*B*), mslo1-K361N,R514N (*C*), and mslo1-R514N (*D*) show the characteristic leftward shift as $Ca^{2+}{}_i$ is switched from 0.3 to 100 μM. Each fitting curve was obtained from averaging $G/G_{max} - V$ data from 3 to 8 patches at each $Ca^{2+}{}_i$. (*E*) At 0.3 μM $Ca^{2+}{}_i$, V_{half} values from mslo1-K361N, R514N ($n = 3$) and mslo1-R514N channels ($n = 5$) are significantly lower than those of WT mslo1 ($n = 9$). At 100 μM $Ca^{2+}{}_i$, V_{half} from mso1-R514N channel ($n = 3$) was significantly lower than those from WT mslo1 ($n = 4$) and mslo1-K361N,R514N ($n = 4$). $^{**}P < 0.01$ vs. WT mslo1 at 0.3 μM $Ca^{2+}{}_i$; $^{\#\#}P < 0.01$ vs. WT mslo1 at 100 μM $Ca^{2+}{}_i$. In *B*–*E*, data are presented at mean ± SEM.

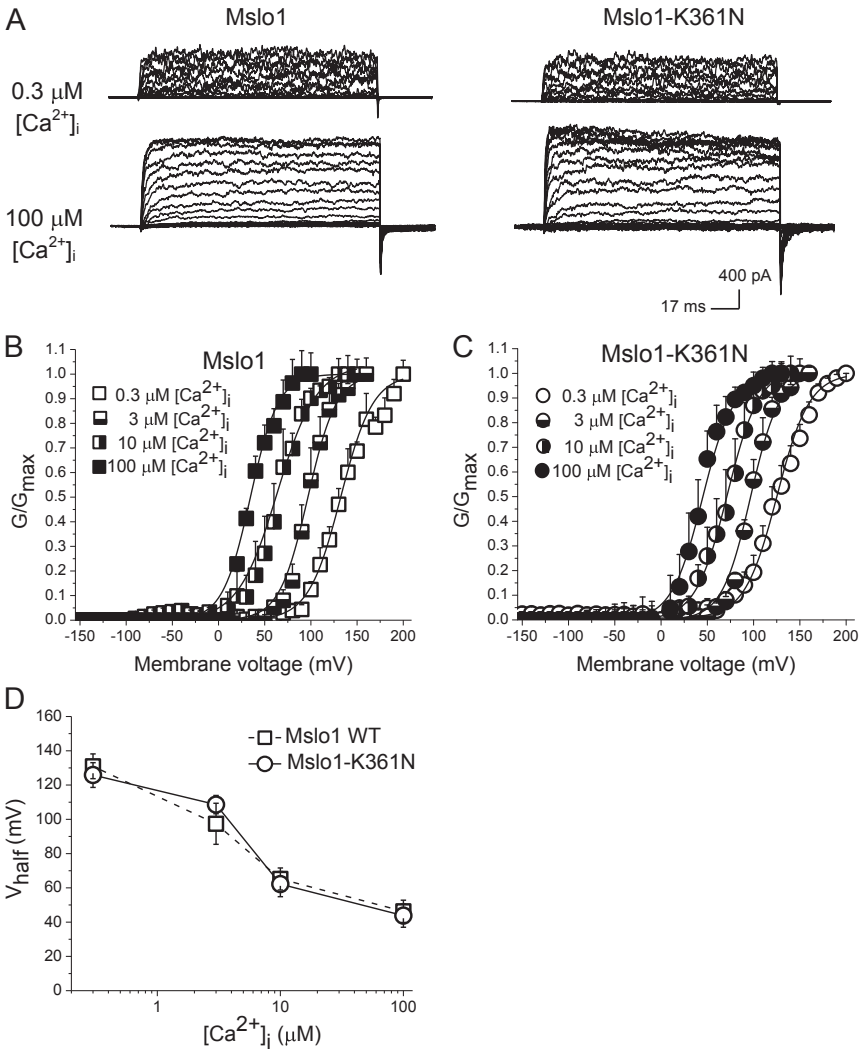

Fig. S4. The K361N substitution in mslo1, which blocks the channel's ethanol sensitivity, does not affect the apparent Ca^{2+} sensitivity. (*A*) Macroscopic current traces from oocyte membrane I/O patches expressing either WT mslo1 or mslo1-K361N and exposed to 0.3 and 100 μM Ca^{2+}_i. $G/G_{max} - V$ plots from mslo1 (*B*) and mslo1-K361N (*C*) show a characteristic progressive leftward shift left as Ca^{2+}_i is stepwise increased from 0.3 to 100 μM. Each fitting curve was obtained from averaging $G/G_{max} - V$ data from 3 to 9 patches at each Ca^{2+}_i. (*D*) V_{half} as function of Ca^{2+}_i from WT mslo1 vs. mslo1-K361N channels are undistinguishable. In *B*–*D*, data are presented at mean ± SEM.

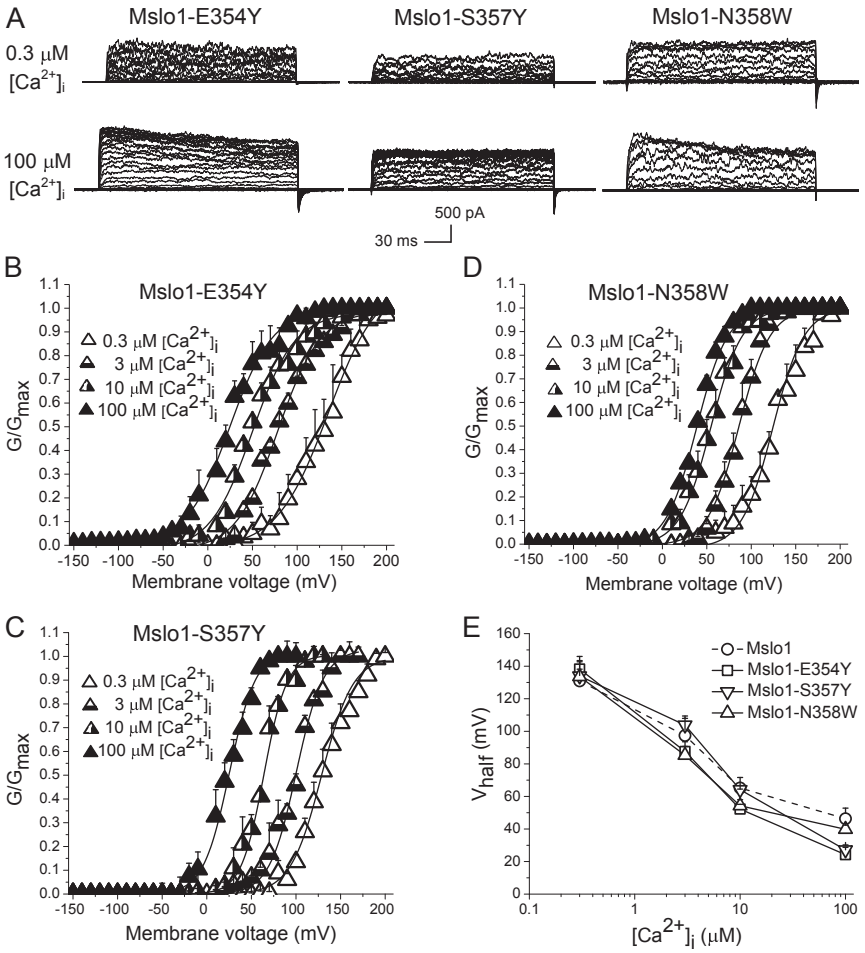

Fig. S5. Bulky substitutions outside the ethanol-sensing pocket do not affect the channel's apparent Ca^{2+} sensitivity. (*A*) Macroscopic currents from oocyte membrane I/O patches expressing either mslo1-E354Y, mslo1-S357Y, or mslo1-N358W and exposed to 0.3 and 100 μM $Ca^{2+}{}_i$. $G/G_{max} - V$ plots from mslo1-E354Y (*B*), mslo1-S357Y (*C*), and mslo1-N358W (*D*) show the characteristic, progressive leftward shift as $Ca^{2+}{}_i$ is stepwise increased from 0.3 to 100 μM. Each fitting curve was obtained from averaging $G/G_{max} - V$ data from 3 to 7 patches at each $Ca^{2+}{}_i$. (*E*) Average ± SEM. V_{half} data as function of $Ca^{2+}{}_i$ from WT mslo1, mslo1-E354Y, mslo1-S357Y, and mslo1-N358W channels are undistinguishable.

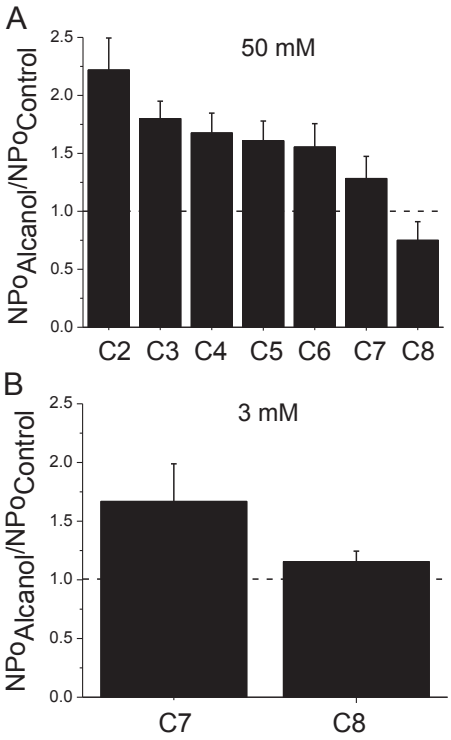

Fig. S6. *N*-alkanol modulation of mslo1 channel NPo presents a "cutoff". (*A*) Averaged data showing increase in mslo1 NPo in response to application of long chain-alkanols (50 mM) to the intracellular side of oocyte membrane I/O patches. C2: ethanol; C3: propanol, C4: butanol, C5: pentanol; C6: hexanol; C7: heptanol; C8: octanol. The differential action of C7 vs. C8 (50 mM) cannot be explain by poor solubility/precipitation of the latter, as such differential outcome is also obtained when both n-alkanols are probed at 3 mM (*B*). Collectively, these data are identical to those previously communicated in intact cells using intracellular, two-microelectrode voltage clamp. In both *A* and *B*, a dashed line indicates the point at which NPo is unchanged by alkanol.